沉积学报
ACTA SEDIMENTOLOGICA SINICA
ISSN 1000-0550
CN 62-1038/P

南华北早二叠世泥岩沉积与深时陆地古温度重建

杨江海，王圆，刘佳，马睿，杜远生，刘超，余文超

引用本文:
杨江海, 王圆, 刘佳, 等. 南华北早二叠世泥岩沉积与深时陆地古温度重建[J]. 沉积学报, 2021, 39(3): 540–549.
YANG JiangHai, WANGYuan, LIU Jia, et al. Early Permian Mudrock Deposits and Deep–time Land Surface Temperature Reconstruction, Southern North China[J]. *Acta Sedimentologica Sinica*, 2021, 39(3): 540–549.

文章编号:1000-0550(2021)03-0540-10 DOI: 10.14027/j.issn.1000-0550.2020.092

南华北早二叠世泥岩沉积与深时陆地古温度重建

杨江海[1,2],王圆[2],刘佳[2],马睿[2],杜远生[1,2],刘超[1],余文超[2]

1.中国地质大学(武汉)生物地质与环境地质国家重点实验室,武汉 430074

2.中国地质大学(武汉)地球科学学院,武汉 430074

摘 要 地球在地质历史时期经历过多次冰室与温室气候状态间的相互转换,也发生了以雪球地球为特征的极冷和以快速升温为特征的极热气候事件。二叠纪是晚古生代冰期到中生代温室气候转换的关键时期。为深入认识二叠纪的重大气候演变,急需解决的一个科学问题是如何获取高精年代地层约束的陆地古气候信息。通过总结近年来报道的华北南部石炭—二叠纪含煤岩系的同位素年代学和泥岩风化地球化学数据,建立了基于高精年代地层格架的化学风化趋势,定量重建了华南南部在约300~286 Ma的陆地古温度变化曲线,揭示了低纬陆地古气候对高纬冰川活动和全球气候变化的响应。新建的南华北陆地古温度曲线指示了与早二叠世Asselian初期和Sakmarian晚期两次冰川消融相对应的气候变暖事件,也指示了与Asselian早期和Artinskian早期两次冰川扩张相对应的气候变冷事件。

关键词 南华北;深时古气候;泥岩;风化地球化学;陆地古温度

第一作者简介 杨江海,男,1984年出生,博士,副教授,沉积地质学,E-mail: yangjh@cug.edu.cn

中图分类号 P532 **文献标志码** A

0 引言

气候是影响人类生存发展的重要自然因素,与社会经济生活息息相关。人类与气候的关系经历了从早期的忍耐抗争,到后来的顺应利用,再到现在的保护维系,而未来社会的发展与气候变化的联系将更加紧密。为准确预测未来气候变化,迫切需要对地球过去的气候历史,包括变化事件及其控制机制进行更为系统的理解和认识[1-3]。美国国家研究理事会在2011年发布了名为“Understanding Earth′s deep past: lessons for our climate future”的调研报告[4],美国国家自然科学基金委在2017年启动了“Paleo Perspectives on Climate Change (P2C2)”研究计划,并在2020年发布了地球科学未来十年的战略报告,提出了12个优先科学问题,其中第8个问题即为“地球的过去揭示了什么样的气候系统和动力机制”。我国学者也较早注意到深时研究的重要性[2,5-6],2016年由中国科学院地学部和国家自然科学基金委联合资助的“中国沉积学发展战略”调研将“深时气候学”列为10个调研主题之一。2019年启动的深时数字地球(DDE)国际大科学计划也将深时古气候演化作为主要的研究目标。

地球自新元古代以来经历了大幅度的气候变化,发生了多次的冰室—温室气候转换和极端气候事件[2-4],后者包括晚新元古代的雪球地球[7]、晚白垩世的温室最暖期[8]、古新世—始新世极热期[9-10]等等,前者包括古新世—渐新世从温室到冰室的转变[11-12]、二叠纪从冰室到温室的转变[13]等等。二叠纪是晚古生代冰期到中生代温室转变的关键时期,高纬冈瓦纳地区出现阶段性冰川活动且冰川规模和强度减弱,气候整体变暖,大气CO_2浓度从约300 mL/m^{3}上升到大于1 000 mL/m^3,代表了地球有陆地植被以来唯一一次冰室—温室气候转换[1,14-15],是认识地球大幅度气候变化、理解气候—冰川—大气CO_2—火山活动相互联系的重要窗口[16-19]。通过二叠纪中—高纬地区冰川沉积记录,前人确定了早二叠世早期的大规模冰川活动和随后东澳大利亚的三次区域/山岳型冰川活动[14-15,20-24](早二叠世晚期、中二叠世中期和晚二

收稿日期:2020-06-16; **收修改稿日期**:2020-10-10

基金项目:国家自然科学基金(41572078,41872106);生物地质与环境地质国家重点实验自主课题(GKZ18Y660,GPMR201609)[**Foundation**: National Natural Science Foundation of China, No. 41572078, 41872106; National Key Experimental Project of Biogeography and Environmental Geology, No. GKZ18Y660, GPMR201609]

叠世早期四次冰川活动),通过海相生物壳氧同位素组成重建了中—低纬地区的海水古温度变化趋势[25-31],但是对陆地古气候的定量研究较少[32],对气候冷暖演变的机制及其与火山活动、化学风化和构造运动的内在联系还存在较大争议[17,19,33]。我们对华北南部晚石炭—早二叠世的泥岩沉积序列开展了详细的年代地层学和沉积风化地球化学研究,提出了定量估算陆地古温度的新方法,识别出早二叠世Asselian早期和Sakmarian晚期的两次变暖事件[34-37]。本文将华北南缘石炭纪末—早二叠世地层的年龄和组成数据进行总结,定量重建了华北南部约300 Ma至286 Ma间的陆地古温度变化曲线。

1　地质背景和采样剖面

在晚石炭—早二叠世时期,华北位于低纬近赤道地区,与Pangea泛大陆之间为特提斯洋所分隔,向东与泛大洋相接[38-42](图1)。华北的晚石炭—早二叠世地层平行不整合覆盖在寒武—奥陶纪碳酸盐岩之上,是一套以细碎屑岩为主夹灰岩和砂岩的含煤岩系,自下而上包括本溪组、太原组和山西组[43-45]。前人对华北太原组的灰岩开展了大量的生物地层学研究,约束其时代为石炭纪末—早二叠世,且具有穿时特征,而最大海泛面出现在太原组底部[46-48],形成泛华北的陆表海沉积。在沉积环境上,本溪组、太原组和山西组整体上具有从陆表海到三角洲转变的特征[45, 49-50],且华北南北两侧毗邻秦岭—大别造山带和兴蒙造山带及隆起区,构成了晚古生代沉积盆地的主要沉积物源区[51-53]。在华北晚石炭—早二叠世地层中夹有多层凝灰岩、凝灰质沉积岩和火山黏土沉积,多为中酸性,是区域地层对比的重要标志层[50, 54-55]。

研究样品采集于华北东南缘豫东永城地区的两个钻孔剖面,即钻孔ZK1401和ZK0901[35]。ZK0901剖面的采样层位为本溪组、太原组和山西组下部,ZK1401剖面的采样层位为山西组中上部和下石盒子组。在采样剖面上,本溪组为灰色—灰白色均质层理泥岩,太原组为生物碎屑灰岩、泥岩和砂岩夹煤层,山西组和下石盒子组为含煤的砂岩和泥岩(图2)。对两个岩芯剖面进行了系统的泥岩样品采集,在显微观察分析基础上开展了XRD(X射线衍射)矿物学、XRF(X荧光光谱)主量元素和ICPMS(电感耦合等离子质谱)微量元素分析;同时,对采集的火山黏土岩、凝灰岩和凝灰质砂岩开展了LA-ICPMS(激光剥蚀电感耦合等离子质谱)和CA-TIMS(化学剥蚀热电离质谱)锆石U-Pb定年。详细的样品描述、分析方法和分析结果已有专门文章[34-35, 37]予以报道。本文将对两个剖面的数据进行综合分析,建立统一的高精年代地层格架,重建华北南部早二叠世的大陆风化趋势和古气候变化。

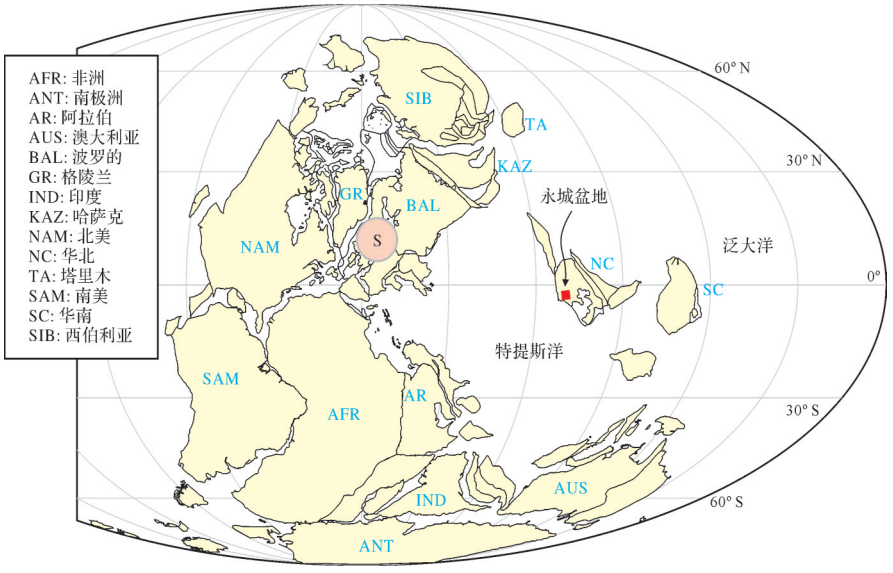

图1　早二叠世早期的全球海陆分布图,红方框指示南华北采样点位置(永城盆地)

Fig.1　Reconstruction of early Permian global paleogeography showing the position of sampled successions in southern North China (red solid square, Yongcheng Basin)

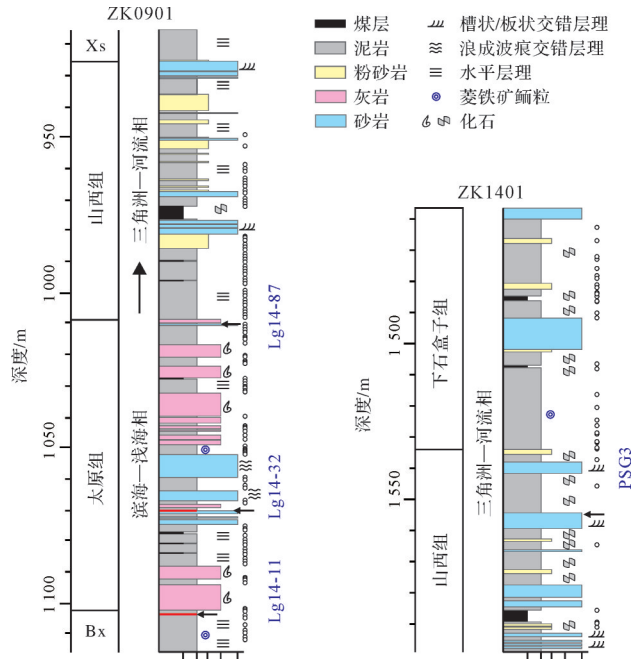

图2 钻孔ZK0901和ZK1401采样柱状图

Fig.2 Sampled successions of two core sections of ZK0901 and ZK1401

2 华北早二叠世沉积序列的高精年代地层格架

前人通过牙形石、蜓类等海相生物化石对华北的石炭—二叠系进行了生物地层学研究[46-47,56-58]，然而由于海相灰岩层发育的不连续性和关键化石种属的缺乏，华北的石炭—二叠系仍缺少精确的时代约束[59]。为进一步确定华北石炭—二叠系的沉积时代，我们对钻孔ZK1401山西组上部的凝灰质砂岩开展了LA-ICPMS锆石U-Pb年龄分析，获得的主要年龄组的加权平均年龄为293±2.5 Ma，代表了该凝灰质岩层的沉积时代[34]，对钻孔ZK0901本溪组顶部的凝灰质黏土岩和太原组中部的凝灰岩及顶部的凝灰质砂岩开展了CA-TIMS锆石U-Pb定年工作，获得了（301.13±0.21）Ma、（299.32±0.35）Ma和（295.65±0.14）Ma三个高精度地层年龄，将太原组的沉积时代约束在晚石炭世Gzhelian晚期到早二叠世Asselian晚期[37]。根据所获得的三个CA-TIMS高精度地层时代和定年样品间的地层厚度，我们获得了3个在误差范围内一致的平均沉积速率，即（17.7±2.2）m/Myr、（16.9±0.7）m/Myr和（16.5±0.6）m/Myr。我们选定（16.9±0.7）m/Myr来代表从本溪组到下石盒子组的整个含煤岩系的平均沉积速率，可以将山西组与下石盒子组的地层界线约束在约291 Ma,这与钻孔ZK1401山西组上部凝灰质砂岩获得的（293±2.5）Ma的锆石年龄，在误差范围内是一致的。因此，利用获得的高精度锆石年龄和（16.9±0.7）m/Myr的平均沉积速率，采用内插法对两个钻孔剖面进行地层时代对比，并建立高精年代地层格架是完全可行的。根据所建立的统一年代地层格架，可将ZK1401和ZK0901两个剖面的采样层位精确限定在约302 Ma至286 Ma之间（图3）。

需要指出，由于从本溪组到下石盒子组发生了从海相到陆相沉积的演化和岩性的变化，因此采用线性内插法来计算地层时代会存在许多误差。尽管如此，在没有更多的高精度同位素年龄和高分辨生物地层学数据的情况下，我们建立的从本溪组到下石盒子组的年代地层格架可以作为区域地层对比、古气候和古地理研究的重要基础。

3 华北早二叠世泥岩沉积与大陆风化趋势

砂岩和泥岩作为最常见的陆源碎屑沉积岩，是陆地表层岩石风化剥蚀和源—汇沉积过程的重要信息载体[6,60-64]。其中，砂岩主要源自陆地岩石的物理侵蚀作用[65-66]，而泥岩则主要为陆地岩石化学风化的产物（如黏土矿物）和泥级碎屑颗粒物质，其矿物和化学组成与源区岩石的化学风化强度具有密切联系[65-66]。前人提出了多种化学风化指标来衡量泥岩源区的化学风化强度，并指出成岩作用、源岩组成、沉积再旋回、水力分选和物理侵蚀等因素会影响泥岩风化地球化学分析的可靠性[63-70]。我们通过综合分析泥岩的矿物学和元素地球化学数据，识别出受碳酸盐化等成岩作用、水力分选作用等强烈影响的样品，结合区域沉积古地理确定了具有华北南缘大陆地壳属性的平均源岩组成，排除了源区物理侵蚀速率对泥岩物质组成变化的影响。为获得可靠的泥岩源区风化趋势，我们采用了多个化学风化指标来约束源区的化学风化强度，如Q/F（石英/长石）比值、Clay/F（黏土矿物/长石）比值、化学蚀变指数[71]（CIA）、Park风化指数[72]（WIP）、Na风化指数[66,73]（α_{Na},α^{Al}_{Na}）、K风化指数[66,73]（α_K,α^{Al}_K）和Na亏损指数[74]（τ_{Na}）等。选用多指标的优势在于：1）不同指标的计算方法不一样，可以降低单指标分析的不确定性；2）不同指标涉及到不同的元素，可以避免因特定元素含量变化引

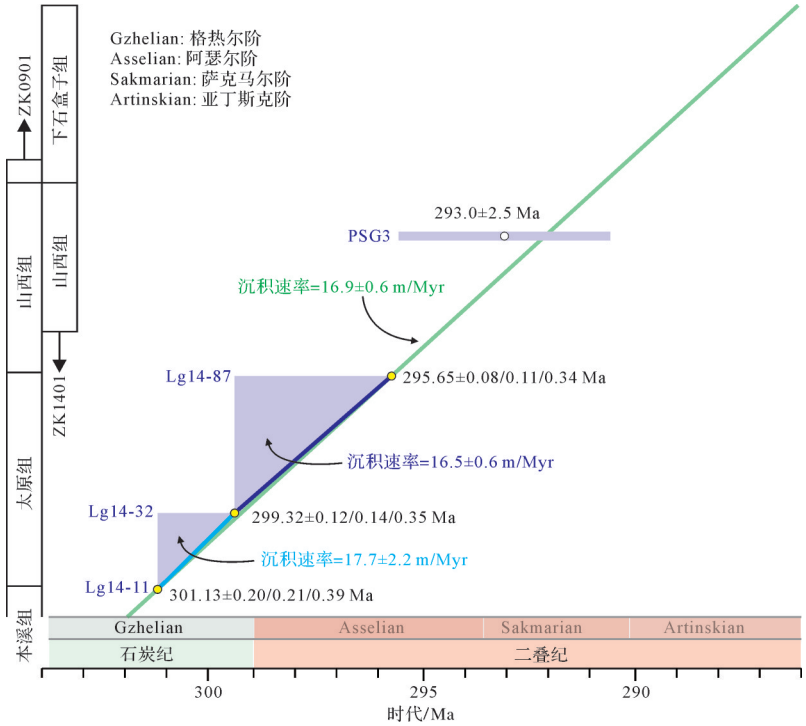

图3　采样层位的高精年代地层格架

平均沉积速率是根据3个CA-TIMS高精度锆石U-Pb年龄[37]计算的,推测的山西组顶部的模式年龄与已有的LA-ICPMS锆石U-Pb年龄[34]一致

Fig.3　High-precision chronostratigraphic framework of the sampled successions

Average depositional rates obtained from three high-precision CA-TIMS zircon U-Pb ages[37]. The modeled age for the top Shanxi Formation is consistent with LA-ICPMS zircon U-Pb ages reported for the upper Shanxi Formation[34]

起的化学风化分析偏差;3)不同指标对风化的敏感性不一样,综合使用多指标可增强化学风化强度分析的有效性[36]。

Yang *et al.*[34-35,37]对这两个剖面的泥岩矿物、地球化学组成进行了系统分析,初步确定了石炭纪末—早二叠世的大陆风化趋势,识别出了早二叠世Asselian早期和Sakmarian晚期的两次化学风化增强事件。在此基础上,本文利用CIA和τ_{Na}两个化学风化指标建立了一个基于高精年代地层格架的华北南缘大陆风化趋势。局部加权回归(LOESS)拟合的化学风化趋势显示,源区化学风化强度在约300~298 Ma发生快速升高而后在约298~296.5 Ma又快速降低,随后保持较低的水平,直到约292~290 Ma发生第二次大幅度升高而后在约290~288 Ma又快速降低,分别在~298 Ma和~290 Ma形成两个高化学风化强度的峰值(图4)。

4　讨论

早二叠世是地球气候快速波动的时期,重要气候事件包括Pangea低纬地区的普遍干旱化[32,75-78]、冈瓦纳地区的冰川大规模消融和阶段性冰川扩张[14-15,24]、大气CO_2浓度的大幅度波动[1]、古海水温度的升高和降低[27-29]等。近年来,冈瓦纳大陆石炭纪末—早二叠世冰川沉积的地层时代已有较好的约束。Stollhofen *et al.*[79]总结了南非冰川石炭—二叠纪冰川沉积地层(Dwyka群)和冰后期地层(Ecca群)的凝灰岩锆石U-Pb年龄,获得了Hardap Shale顶部和Ecca群底部的时代分别为297.1±1.8 Ma和290.9±1.7 Ma两个年龄,约束了早二叠世Asselian初期和Sakmarian晚期的两次大规模冰川消融事件。在Dwyka群的冰川沉积序列中,Hardap Shale代表了第三个冰川消融沉积旋回的上部序列,其顶部最新的高精度锆石U-Pb年龄为~296.5 Ma[80]。通过对南美洲Paraná盆地冰后期Guatá群底部凝灰岩进行CA-TIMS锆石U-Pb定年,Griffis *et al.*[81]获得了一组~298 Ma的高精度地层年龄,将Itararé群顶部(Taciba组)冰川大规模消融的时间约束在为石炭纪末—二叠纪初。Griffis *et al.*[80]认为,南非Dwyka群的Hardap Shale对应于南美冰后期Rio Bonito组的中部泥岩。但南非的Hardap Shale与南美的Taciba组上部具有一致的海

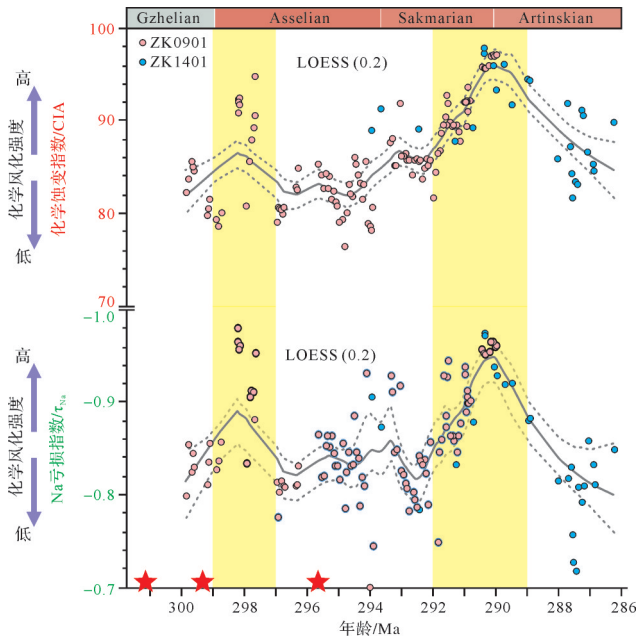

图4 化学风化指数(CIA)和Na亏损指数(τ_{Na})随时间的变化,指示了南华北在石炭纪末—早二叠世的大陆化学风化趋势,黄色阴影区指示了早二叠世的两次强化学风化时期

Fig.4 Temporal variations in CIA and τ_{Na} values, indicating continental chemical weathering trends of southern North China in the End Carboniferous-Early Permian Period

相生物化石组合[82],且~297 Ma的锆石U-Pb年龄仅限定了Hardap Shale的顶部时代,其底部可能延伸至石炭—二叠纪界线[79]。因此,Hardap Shale很可能对应于Taciba组上部—Rio Bonito组下部,共同代表石炭—二叠纪界线附近的大规模冰川消融和海平面上升事件[37]。Garbelli *et al.*[21]测定了澳大利亚东部悉尼盆地早二叠世冰川沉积序列中腕足壳的$^{87}Sr/^{86}Sr$比值,利用与海水Sr同位素曲线对比的方法,确定了Wasp Head组上部地层时代为约(289.6±1.5) Ma,代表了早二叠世P1与P2冰川活动期[14]之间冰川消融事件的晚期年龄。

本文建立了华北南部早二叠世高精年代地层格架和高分辨率大陆风化趋势,与高纬冈瓦纳地区的冰川型沉积记录具有很好的对比关系(图5)。其中,最为显著的是:1)华北大陆化学风化强度在约300~298 Ma显著升高,对应于南美和南非地区记录的石炭纪末—二叠纪初的大规模冰川消融;2)华北大陆风化强度在约298~297 Ma快速降低,并在约296.5 Ma达到最低值,对应于南非和东澳地区Asselian冰川沉积的重新启动;3)华北大陆风化强度在约296.5~292 Ma整体保持低值,对应于冈瓦纳大陆Asselian期—Sakmarian早期的大规模冰川活动;4)华北大陆化学风化强度在约292~290 Ma显著升高,对应于冈瓦纳大陆在Skamarian晚期的大规模冰川消融;5)华北大陆风化强度后在Artinskian早期又快速降低至Asselian冰川期的低值水平,对应于东澳大利亚P2冰川沉积的启动。这一耦合关系表明,华北的大陆化学风化趋势反应了全球气候的冷、暖变化,而没有受到构造活动和物理侵蚀速率变化的影响。对现代关键带的化学风化研究指出,在供应限制型风化机制下,岩石化学风化速率与物理侵蚀速率成正比,而化学风化强度则主要与气候条件有关[6,83-84]。Yang *et al.*[35]收集整理了现代中—低纬地区花岗质基岩的化学风化数据,发现在年降雨量>400 mm的中—低等物理侵蚀(物理侵蚀速率小于100 m/Myr)地区,其表层土壤的化学风化强度τ_{Na}与陆地温度MAT成正相关关系,即$MAT=-24.2\times\tau_{Na}-0.9$。考虑到我们研究的华北南部石炭纪末—早二叠世的泥岩均沉积于滨海—三角洲环境,其物质组成反应了物源区表层土壤化学风化强度的平均值,因此可作为大区域陆地表层古温度的定量指标。利用MAT-τ_{Na}转换方程和计算获得的泥岩τ_{Na}值,我们定量重建了华北南部石炭纪末—早二叠世早期(约300~286 Ma)的陆地表层古温度,其变化范围为18.5 ℃~23 ℃(图5)。

根据这一陆地古温度变化曲线和冈瓦纳冰川型沉积序列,地球在~298 Ma和~290 Ma形成两个持续时间为约1~2 Ma的、与冰川消融相对应的气候暖期。与温室气候条件下的极热事件不同[8-10],~298 Ma和~290 Ma的气候暖期代表了冰室气候期的快速变暖事件,对认识地球气候系统演化、理解气候变化—冰川活动—火山喷发的内在联系具有重要意义。Yang *et al.*[37]认为~298 Ma的气候暖期与Skagerrak大火成岩省快速CO_2温室气体释放有关,但~290 Ma气候暖期及之后气候变冷和冰川活动的形成机制仍未有深入研究,可能与同时期的塔里木大火成岩省[85-86]和Panjal大火成岩省[87-88]等大规模火山活动有关。

5 结论

本文系统总结了华北南部从本溪组、太原组、山西组到下石盒子组的同位素时代和泥岩风化地球化学数据,建立了石炭纪末—早二叠世(~302~286 Ma)的高精度年代地层格架,揭示了这一时期华北南缘

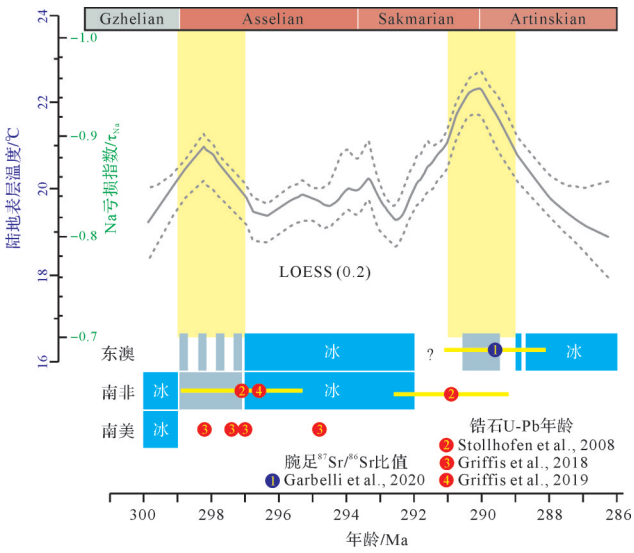

图5　南华北石炭纪末—早二叠世化学风化趋势和陆地表层古温度变化与高纬冈瓦纳冰川型沉积记录对比图，黄色阴影区指示了早二叠世的两次强化学风化时期，黄色短线指示地层年龄误差

Fig.5　Correlations of the End Carboniferous-Early Permian chemical weathering trends and land surface paleotemperatures in southern North China, with time-equivalent glacial-deglacial sedimentary records in high-latitude Gondwana continents

陆地表层的化学风化趋势。华北南部石炭纪末—早二叠世滨海泥岩记录的陆地化学风化趋势与高纬冈瓦纳冰川型沉积序列具有很好的对比关系，即化学风化强度的升高和降低分别对应于冰川的消融和扩张。利用前人提出的MAT(陆地表层温度)-τ_{Na}(化学风化强度)转换方程，我们定量重建了华北南部在约300~286 Ma的陆地表层温度变化曲线，揭示早二叠世低纬地区陆地古温度对两次冰川消融和冰川扩张事件的响应。

参考文献(References)

[1] Montañez I P, Tabor N J, Niemeier D, et al. CO_2-forced climate and vegetation instability during Late Paleozoic deglaciation[J]. Science, 2007, 315(5808): 87-91

[2] 孙枢,王成善. "深时"(Deep Time)研究与沉积学[J]. 沉积学报, 2009, 27(5): 792-810. [Sun Su, Wang Chengshan. Deep time and sedimentology[J]. Acta Sedimentologica Sinica, 2009, 27(5): 792-810.]

[3] Parrish J T, Soreghan G S. Sedimentary geology and the future of paleoclimate studies[J]. The Sedimentary Record, 2013, 11: 4-10.

[4] NRC. Understanding Earth's deep past: Lessons for our climate future[M]. Washington, D. C.: The National Academies Press, 2011: 1-208.

[5] 王成善,王天天,陈曦,等. 深时古气候对未来气候变化的启示[J]. 地学前缘, 2017, 24(1): 1-17. [Wang Chengshan, Wang Tiantian, Chen Xi, et al. Paleoclimate implications for future climate change[J]. Earth Science Frontiers, 2017, 24(1): 1-17.]

[6] 杨江海,马严. 源—汇沉积过程的深时古气候意义[J]. 地球科学, 2017, 42(11): 1910-1921. [Yang Jianghai, Ma Yan. Paleoclimate perspectives of source- to-sink sedimentary processes[J]. Earth Science, 2017, 42(11): 1910-1921.]

[7] Hoffman P F, Kaufman A J, Halverson G P, et al. A Neoproterozoic snowball Earth[J]. Science, 1998, 281(5381): 1342-1246.

[8] Klages J P, Salzmann U, Bickert T, et al. Temperate rainforests near the South Pole during peak Cretaceous warmth[J]. Nature, 2020, 580(7801): 81-86.

[9] Robert C, Kennett J P. Antarctic subtropical humid episode at the Paleocene-Eocene boundary: Clay-mineral evidence[J]. Geology, 1994, 22(3): 211-214.

[10] Weijers J W H, Schouten S, Sluijs A, et al. Warm arctic continents during the Palaeocene-Eocene thermal maximum[J]. Earth and Planetary Science Letters, 2007, 261(1/2): 230-238.

[11] Liu Z H, Pagani M, Zinniker D, et al. Global cooling during the Eocene-Oligocene climate transition[J]. Science, 2009, 323(5918): 1187-1190.

[12] Robert C, Kennett J P. Antarctic continental weathering changes during Eocene-Oligocene cryosphere expansion: Clay mineral and oxygen isotope evidence[J]. Geology, 1997, 25(7): 587-590.

[13] Montañez I P, Poulsen C J. The Late Paleozoic Ice Age: An evolving paradigm[J]. Annual Review of Earth and Planetary Sciences, 2013, 41: 629-656.

[14] Fielding C R, Frank T D, Birgenheier L P, et al. Stratigraphic imprint of the Late Palaeozoic Ice Age in eastern Australia: A record of alternating glacial and nonglacial climate regime[J]. Journal of the Geological Society, 2008, 165(1): 129-140.

[15] Isbell J L, Henry L C, Gulbranson E L, et al. Glacial paradoxes during the Late Paleozoic Ice Age: Evaluating the equilibrium line altitude as a control on glaciation[J]. Gondwana Research, 2012, 22(1): 1-19.

[16] Yang J H, Cawood P A, Du Y S. Voluminous silicic eruptions during Late Permian Emeishan igneous province and link to climate cooling[J]. Earth and Planetary Science Letters, 2015, 432: 166-175.

[17] Soreghan G S, Soreghan M J, Heavens N G. Explosive volcanism as a key driver of the Late Paleozoic Ice Age[J]. Geology, 2019, 47(7): 600-604.

[18] Yang J H, Cawood P A, Du Y S, et al. Early Wuchiapingian cooling linked to Emeishan basaltic weathering?[J]. Earth and Planetary Science Letters, 2018, 492: 102-111.

[19] McKenzie N R, Horton B K, Loomis S E, et al. Continental

arc volcanism as the principal driver of icehouse-greenhouse variability[J]. Science, 2016, 352(6284): 444-447.

[20] Metcalfe I, Crowley J L, Nicoll R S, et al. High-precision U-Pb CA-TIMS calibration of Middle Permian to Lower Triassic sequences, mass extinction and extreme climate-change in eastern Australian Gondwana[J]. Gondwana Research, 2015, 28(1): 61-81.

[21] Garbelli C, Shen S Z, Immenhauser A, et al. Timing of Early and Middle Permian deglaciation of the southern hemisphere: Brachiopod-based $^{87}Sr/^{86}Sr$ calibration[J]. Earth and Planetary Science Letters, 2019, 516: 122-135.

[22] Isbell J L, Koch Z J, Szablewski G M, et al. Permian glacigenic deposits in the Transantarctic Mountains, Antarctica[M]// Fielding C R, Frank T D, Isbell J L. Resolving the Late Paleozoic ice age in time and space. Boulder, America: Geological Society of America, 2008: 59-70.

[23] Isbell J L, Cole D I, Catuneanu O. Carboniferous-Permian glaciation in the main Karoo Basin, South Africa: Stratigraphy, depositional controls, and glacial dynamics[M]//Fielding C R, Frank T D, Isbell J L. Resolving the Late Paleozoic ice age in time and space. Boulder, America: Geological Society of America, 2008: 71-82.

[24] Fielding C R, Frank T D, Isbell J L. The Late Paleozoic Ice Age—A review of current understanding and synthesis of global climate patterns[M]//Fielding C R, Frank T D, Isbell J L. Resolving the Late Paleozoic ice age in time and space. Boulder, America: Geological Society of America, 2008: 343-354.

[25] Angiolini L, Jadoul F, Leng M J, et al. How cold were the Early Permian glacial tropics? Testing sea-surface temperature using the oxygen isotope composition of rigorously screened brachiopod shells[J]. Journal of the Geological Society, 2009, 166(5): 933-945.

[26] Grossman E L, Yancey T E, Jones T E, et al. Glaciation, aridification, and carbon sequestration in the Permo-Carboniferous: The isotopic record from low latitudes[J]. Palaeogeography, Palaeoclimatology, Palaeoecology, 2008, 268(3/4): 222-233.

[27] Korte C, Jasper T, Kozur H W, et al. $\delta^{18}O$ and $\delta^{13}C$ of Permian brachiopods: A record of seawater evolution and continental glaciation[J]. Palaeogeography, Palaeoclimatology, Palaeoecology, 2005, 224(4): 333-351.

[28] Korte C, Jones P J, Brand U, et al. Oxygen isotope values from high-latitudes: Clues for Permian sea-surface temperature gradients and Late Palaeozoic deglaciation[J]. Palaeogeography, Palaeoclimatology, Palaeoecology, 2008, 269(1/2): 1-16.

[29] Chen B, Joachimski M M, Shen S Z, et al. Permian ice volume and palaeoclimate history: Oxygen isotope proxies revisited[J]. Gondwana Research, 2013, 24(7): 77-89.

[30] Beard J A, Ivany L C, Runnegar B. Gradients in seasonality and seawater oxygen isotopic composition along the Early Permian Gondwanan coast, SE Australia[J]. Earth and Planetary Science Letters, 2015, 425: 219-231.

[31] Wang W Q, Garbelli C, Zhang F F, et al. A high-resolution Middle to Late Permian paleotemperature curve reconstructed using oxygen isotopes of well-preserved brachiopod shells[J]. Earth and Planetary Science Letters, 2020, 540: 116245.

[32] Tabor N J, DiMichele W A, Montañez I P, et al. Late Paleozoic continental warming of a cold tropical basin and floristic change in western Pangea[J]. International Journal of Coal Geology, 2013, 119: 177-186.

[33] Goddéris Y, Donnadieu Y, Carretier S, et al. Onset and ending of the Late Palaeozoic ice age triggered by tectonically paced rock weathering[J]. Nature Geoscience, 2017, 10(5): 382-386.

[34] Yang J H, Cawood P A, Du Y S, et al. Global continental weathering trends across the Early Permian glacial to postglacial transition: Correlating high- and low- paleolatitude sedimentary records[J]. Geology, 2014, 42(10): 835-838.

[35] Yang J H, Cawood P A, Du Y S, et al. Reconstructing Early Permian tropical climates from chemical weathering indices[J]. GSA Bulletin, 2016, 128(5/6): 739-751.

[36] Yang J H, Du Y S. Weathering geochemistry and palaeoclimate implication of the Early Permian mudstones from eastern Henan province, North China[J]. Journal of Palaeogeography, 2017, 6(4): 370-380.

[37] Yang J H, Cawood P A, Montañez I P, et al. Enhanced continental weathering and large igneous province induced climate warming at the Permo-Carboniferous transition[J]. Earth and Planetary Science Letters, 2020, 534: 116074.

[38] Torsvik T H, van der Voo R, Doubrovine P V, et al. Deep mantle structure as a reference frame for movements in and on the Earth[J]. Proceedings of the National Academy of Sciences of the United States of America, 2014, 111(24): 8735-8740.

[39] Cawood P A, Wang Y J, Xu Y J, et al. Locating South China in Rodinia and Gondwana: A fragment of greater India lithosphere?[J]. Geology, 2013, 41(8): 903-906.

[40] Embleton B J J, McElhinny M W, Ma X H, et al. Permo-Triassic magnetostratigraphy in China: The type section near Taiyuan, Shanxi province, North China[J]. Geophysical Journal International, 1996, 126(2): 382-388.

[41] 朱鸿,杨关秀,盛阿兴. 河南禹州大风口剖面二叠纪地层古地磁研究[J]. 地质学报, 1996, 70(2): 121-128. [Zhu Hong, Yang Guanxiu, Sheng Axing. A study on palaeomagnetism of Permian strata in the Dafengkou section, Yuzhou, Henan province[J]. Acta Geologica Sinica, 1996, 70(2): 121-128.]

[42] Huang B C, Yan Y G, Piper J D A, et al. Paleomagnetic constraints on the paleogeography of the East Asian blocks during Late Paleozoic and Early Mesozoic times[J]. Earth-Science Reviews, 2018, 186: 8-36.

[43] 张泓. 山西大宁盆地晚古生代煤系岩石地层划分与对比[J]. 地层学杂志,1989,13(4):279-289.[Zhang Hong. Division and correlation of the Permo-Carboniferous coal-bearing lithostratigraphy in Datong-Ningwu Basin, Shanxi province[J]. Journal of Stratigraphy, 1989, 13(4): 279-289.]

[44] 裴放. 河南省华北型石炭—二叠纪地层多重划分与对比[J]. 河南地质,1998,16(4):273-280.[Pei Fang. North China type Permo-Carboniferous multiple stratigraphic division and correlation in Henan province[J]. Henan Geology, 1998, 16(4): 273-280.]

[45] 王鸿桢,楚旭春,刘本培,等. 中国古地理图集[M]. 北京:地图出版社,1985:1-283.[Wang Hongzhen, Chu Xuchun, Liu Benpei, et al. Atlas of the palaeogeography of China[M]. Beijing: Cartographic Publishing House, 1985: 1-283.]

[46] 王志浩,祁玉平. 我国北方石炭—二叠系牙形刺序列再认识[J]. 微体古生物学报,2003,20(3):225-243.[Wang Zhihao, Qi Yuping. Review of Carboniferous-Permian conodont biostratigraphy in North China[J]. Acta Micropalaeontologica Sinica, 2003, 20(3): 225-243.]

[47] 万世禄,丁惠. 华北地台石炭、二叠纪牙形石研究新发现及其地质意义[J]. 煤炭学报,1987(1):13-16.[Wan Shilu, Ding Hui. New discovery in the study of Permo-Carboniferous conodonts in North China Platform and its geological significance[J]. Journal of China Coal Society, 1987(1): 13-16.]

[48] Wang Y, Yang J, Ma R, et al. Age constraint on the Lower Taiyuan Formation in southern North China and its paleogeographic implication[J]. submitted, 2020.

[49] 张泓,沈光隆,何宗莲. 华北板块晚古生代古气候变化对聚煤作用的控制[J]. 地质学报,1999,73(2):131-139.[Zhang Hong, Shen Guanglong, He Zonglian. Control of palaeoclimatic change on Late Palaeozoic coal accumulation of the North China Plate[J]. Acta Geologica Sinica, 1999, 73(2): 131-139.]

[50] 钟蓉,孙善平,付泽明. 山东及邻区晚石炭世-早二叠世火山事件沉积及地层对比[J]. 地质学报,1996,70(2):142-152.[Zhong Rong, Sun Shanping, Fu Zeming. Volcanic event deposits and stratigraphic correlation of the Late Carboniferous-Early Permian in Shangdong and adjacent regions[J]. Acta Geologica Sinica, 1996, 70(2): 142-152.]

[51] 李洪颜,徐义刚,黄小龙,等. 华北克拉通北缘晚古生代活化:山西宁武—静乐盆地上石炭统太原组碎屑锆石U-Pb测年及Hf同位素证据[J]. 科学通报,2009,54(5):632-640.[Li Hongyan, Xu Yigang, Huang Xiaolong, et al. Activation of northern margin of the North China Craton in Late Paleozoic: Evidence from U-Pb dating and Hf isotopes of detrital zircons from the Upper Carboniferous Taiyuan Formation in the Ningwu-Jingle Basin[J]. Chinese Science Bulletin, 2009, 54(5): 632-640.]

[52] 马收先,李增学,吕大炜. 南华北石炭—二叠系陆表海层序古地理演化[J]. 沉积学报,2010,28(3):497-508.[Ma Shouxian, Li Zengxue, Lü Dawei. Sequence paleogeographical evolution of epicontinental deposit of Permo-Carboniferous in southern North China[J]. Acta Sedimentologica Sinica, 2010, 28(3): 497-508.]

[53] Zhu X Q, Zhu W B, Ge R F, et al. Late Paleozoic provenance shift in the south-central North China Craton: Implications for tectonic evolution and crustal growth[J]. Gondwana Research, 2014, 25(1): 383-400.

[54] 周安朝,贾炳文,马美玲,等. 华北板块北缘晚古生代火山事件沉积的全序列及其主要特征[J]. 地质论评,2001,47(2):175-183.[Zhou Anchao, Jia Bingwen, Ma Meiling, et al. The whole sequences of volcanic event deposits on the north margin of the North China Plate and their features[J]. Geological Review, 2001, 47(2): 175-183.]

[55] 张开均. 华北板块东缘晚古生代火山活动及其大地构造含义[J]. 中国煤田地质,1998,10(3):10-11,20.[Zhang Kaijun. Late andesitic volcanism of Late Palacozoic Era along the eastern margin of North China Plate and its tectonic implications[J]. Coal Geology of China, 1998, 10: 10-11, 20.]

[56] 宋俊俊,宋慧波,胡斌. 豫西北太原组的时代:来自蜓类化石的证据[J]. 微体古生物学报,2014,31(2):190-204.[Song Junjun, Song Huibo, Hu Bin. Geologic age of the Taiyuan Formation in northwest Henan province: Evidences from fusulinids (foraminifera)[J]. Acta Micropalaeontologica Sinica, 2014, 31(2): 190-204.]

[57] 高莲凤,丁惠,万晓樵. 豫淮盆地太原组顶部斯威特刺(*Sweetognathus*)种的分类修正及其地层意义[J]. 微体古生物学报,2005,22(4):370-382.[Gao Lianfeng, Ding Hui, Wan Xiaoqiao. Taxonomic revision of conodont *Sweetognathus* species in the uppermost Taiyuan Formation, Yuhuai Basin and its significance[J]. Acta Micropalaeontologica Sinica, 2005, 22(4): 370-382.]

[58] 裴放. 河南省华北型石炭纪—二叠纪蜓和牙形石生物地层[J]. 地层学杂志,2004,28(4):344-353.[Pei Fang. The North China type Permo-Carboniferous fusulinid and conodont biostratigraphic units of Henan province[J]. Journal of Stratigraphy, 1998, 28(4): 344-353.]

[59] 沈树忠,张华,张义春,等. 中国二叠纪综合地层和时间框架[J]. 中国科学:地球科学,2019,49(1):160-193.[Shen Shuzhong, Zhang Hua, Zhang Yicun, et al. Permian integrative stratigraphy and timescale of China[J]. Science China: Earth Sciences, 2019, 49(1): 160-193.]

[60] Nesbitt H W, Young G M. Early Proterozoic climates and plate motions inferred from major element chemistry of lutites[J]. Nature, 1982, 299(5885): 715-717.

[61] 杨守业,韦刚健,石学法. 地球化学方法示踪东亚大陆边缘源汇沉积过程与环境演变[J]. 矿物岩石地球化学通报,2015,34(5):902-910.[Yang Shouye, Wei Gangjian, Shi Xuefa. Geochemical approaches of tracing source-to-sink sediment processes and environmental changes at the East Asian continental margin[J]. Bulletin of Mineralogy, Petrology and Geochemistry,

2015, 34(5): 902-910.]

[62] Clift P D, Hodges K V, Heslop D, et al. Correlation of Himalayan exhumation rates and Asian monsoon intensity[J]. Nature Geoscience, 2008, 1(12): 875-880.

[63] Nesbitt H W, Young G M, McLennan S M, et al. Effects of chemical weathering and sorting on the petrogenesis of siliciclastic sediments, with implications for provenance studies[J]. The Journal of Geology, 1996, 104(5): 525-542.

[64] Nesbitt H W, Young G M. Petrogenesis of sediments in the absence of chemical weathering: Effects of abrasion and sorting on bulk composition and mineralogy[J]. Sedimentology, 1996, 43(2): 341-358.

[65] Nesbitt H W, Fedo C M, Young G M. Quartz and feldspar stability, steady and non-steady-state weathering, and petrogenesis of siliciclastic sands and mud[J]. The Journal of Geology, 1997, 105(2): 173-191.

[66] Garzanti E, Padoan M, Setti M, et al. Weathering geochemistry and Sr-Nd fingerprints of equatorial upper Nile and Congo muds[J]. Geochemistry, Geophysics, Geosystems, 2013, 14(2): 292-316.

[67] McLennan S M, Hemming S, McDaniel D K, et al. Geochemical approaches to sedimentation, provenance, and tectonics[M]//Johnsson M J, Basu A. Processes controlling the composition of clastic sediments. Boulder, America: Geological Society of America, 1993: 21-40.

[68] Govin A, Holzwarth U, Heslop D, et al. Distribution of major elements in Atlantic surface sediments (36°N-49°S): Imprint of terrigenous input and continental weathering[J]. Geochemistry, Geophysics, Geosystems, 2012, 13(1): Q01013.

[69] Buggle B, Glaser B, Hambach U, et al. An evaluation of geochemical weathering indices in loess-paleosol studies[J]. Quaternary International, 2011, 240(1/2): 12-21.

[70] Fedo C M, Nesbitt H W, Young G M. Unraveling the effects of potassium metasomatism in sedimentary rocks and paleosols, with implications for paleoweathering conditions and provenance[J]. Geology, 1995, 23(10): 921-924.

[71] Nesbitt H W, Young G M. Prediction of some weathering trends of plutonic and volcanic rocks based on thermodynamic and kinetic considerations[J]. Geochimica et Cosmochimica Acta, 1984, 48(7): 1523-1534.

[72] Parker A. An index of weathering for silicate rocks[J]. Geological Magazine, 1970, 107(6): 501-504.

[73] Gaillardet J, Dupré B, Allegrè C J. Geochemistry of large river suspended sediments: Silicate weathering or recycling tracer?[J]. Geochimica et Cosmochimica Acta, 1999, 63(23/24): 4037-4051.

[74] Rasmussen C, Brantley S, deB. Richter D, et al. Strong climate and tectonic control on plagioclase weathering in granitic terrain[J]. Earth and Planetary Science Letters, 2011, 301(3/4): 521-530.

[75] Tabor N J, Poulsen C J. Palaeoclimate across the Late Pennsylvanian-Early Permian tropical palaeolatitudes: A review of climate indicators, their distribution, and relation to palaeophysiographic climate factors[J]. Palaeogeography, Palaeoclimatology, Palaeoecology, 2008, 268(3/4): 293-310.

[76] Tabor N J, Montanez I P, Scotese C R, et al. Paleosol archives of environmental and climatic history in paleotropical western Pangea during the Latest Pennsylvanian through Early Permian[M]//Fielding C R, Frank T D, Isbell J I. Resolving the Late Paleozoic ice age in time and space. Boulder, America: Geological Society of America, 2008: 291-303.

[77] Michel L A, Tabor N J, Montañez I P, et al. Chronostratigraphy and paleoclimatology of the Lodève Basin, France: Evidence for a pan-tropical aridification event across the Carboniferous-Permian boundary[J]. Palaeogeography, Palaeoclimatology, Palaeoecology, 2015, 430: 118-131.

[78] Kessler J L P, Soreghan G S, Wacker H J. Equatorial aridity in western Pangea: Lower Permian loessite and dolomitic paleosols in northeastern New Mexico, U. S. A.[J]. Journal of Sedimentary Research, 2001, 71(5): 817-832.

[79] Stollhofen H, Werner M, Stanistreet I G, et al. Single-zircon U-Pb dating of Carboniferous-Permian tuffs, Namibia, and the intercontinental deglaciation cycle framework[M]//Fielding C R, Frank T D, Isbell J L. Resolving the Late Paleozoic ice age in time and space. Boulder, America: Geological Society of America, 2008: 83-96.

[80] Griffis N P, Montanez I P, Mundil R, et al. Coupled stratigraphic and U-Pb zircon age constraints on the Late Paleozoic icehouse-to-greenhouse turnover in south-central Gondwana[J]. Geology, 2019, 47(12): 1146-1150.

[81] Griffis N P, Mundil R, Montañez I P, et al. A new stratigraphic framework built on U-Pb single-zircon TIMS ages and implications for the timing of the penultimate icehouse (Paraná Basin, Brazil)[J]. GSA Bulletin, 2018, 130(5/6): 848-858.

[82] Taboada A C, Neves J P, Weinschütz L C, et al. *Eurydesma-Lyonia* fauna (Early Permian) from the Itararé group, Paraná Basin (Brazil): A paleobiogeographic W-E trans-Gondwanan marine connection[J]. Palaeogeography, Palaeoclimatology, Palaeoecology, 2016, 449: 431-454.

[83] Riebe C S, Kirchner J W, Finkel R C. Erosional and climatic effects on long-term chemical weathering rates in granitic landscapes spanning diverse climate regimes[J]. Earth and Planetary Science Letters, 2004, 224(3/4): 547-562.

[84] Ferrier K L, Riebe C S, Hahm W J. Testing for supply-limited and kinetic-limited chemical erosion in field measurements of regolith production and chemical depletion[J]. Geochemistry, Geophysics, Geosystems, 2016, 17(6): 2270-2285.

[85] Xu Y G, Wei X, Luo Z Y, et al. The Early Permian Tarim large igneous province: Main characteristics and a plume incubation model[J]. Lithos, 2014, 204: 20-35.

[86] Yang S F, Chen H L, Li Z L, et al. Early Permian Tarim Large Igneous province in northwest China[J]. Science China Earth Sciences, 2013, 56(12): 2015-2016.
[87] Shellnutt J G. The Panjal traps[M]//Sensarma S, Storey B C. Large igneous provinces from Gondwana and adjacent regions. London: The Geological Society of London, 2018: 59-86.
[88] Shellnutt J G, Bhat G M, Brookfield M E, et al. No link between the Panjal Traps (Kashmir) and the Late Permian[J]. Geophysical Research Letters, 2011, 38(19): L19308.

Early Permian Mudrock Deposits and Deep-time Land Surface Temperature Reconstruction, Southern North China

YANG JiangHai[1,2], WANGYuan[2], LIU Jia[2], MA Rui[2], DU YuanSheng[1,2], LIU Chao[1], YU WenChao[2]

1. State Key Laboratory of Biogeology and Environmental Geology, China University of Geosciences(Wuhan), Wuhan 430074, China

2. School of Earth Sciences, China University of Geosciences(Wuhan), Wuhan 430074, China

Abstract: Earth has experienced multiple greenhouse and icehouse periods and their inter-transformations, and extreme climatic events (e.g., 'snowball' Earth, hyperthermal hothouse) in its geological past. The Permian was a critical period for the evolution from the late Paleozoic ice age to the Mesozoic greenhouse. One of the main challenges to understanding climate evolution in the Permian has been the acquisition of high-precision age-constrained quantitative data regarding successive paleoclimate changes. This work reviews geochronological and geochemical weathering data reported in recent studies of Permo-Carboniferous coal-bearing successions in southern North China. From this data, a high-precision chronostratigraphic framework is established for strata from the Benxi Formation through to the Taiyuan and Shanxi to Xiashihezi Formations, tracking chemical weathering trends in mudrock-source regions in southern North China. The weathering trends correlate very well with the glacial-deglacial sequence in high-latitude Gondwana continents. The proposed land surface MAT (mean temperature) - τ_{Na} (sodium depletion index) transfer function reconstructs the MAT variations for southern North China in the time interval ~300-286 Ma. The MAT curve reflects climate warming during the earliest Asselian and late Sakmarian deglaciations, and indicates climate cooling with the initiation of the Asselian and subsequent Artinskian glaciations.

Key words: southern North China; deep-time paleoclimate; mudrock; weathering geochemistry; land surface paleotemperature